Preferential Solvation and Self-Association in Alcohol−Acetonitrile Mixtures Observed through Mass Spectrometric Analysis of Clusters: Influence of Alkyl Chain Length

Federico Rastrelli,[†] Giacomo Saielli,[‡] and Alessandro Bagno*[,†]

Department of Chemistry, University of Padova, via Marzolo 1, 35131 Padova, Italy, and Institute of Membrane Technology-CNR, Padova Section, via Marzolo 1, 35131 Padova, Italy

Akihiro Wakisaka*

National Institute of Advanced Industrial Science and Technology (AIST), Onogawa 16-1, Ibaraki 305-8569, Tsukuba, Japan

Received: November 11, 2003; In Final Form: January 19, 2004

Molecular clusters formed by fragmentation of liquid droplets of alcohol (methanol or *n*-butanol)−acetonitrile mixtures have been detected and analyzed by means of a specially designed mass spectrometer. In the methanol−acetonitrile mixture, methanol clusters retain a sizable magnitude through most of the composition range, whereas acetonitrile clusters decrease in intensity upon increasing the concentration of methanol. Hydrogen bonding among methanol molecules controls the clustering. On the other hand, in *n*-butanol−acetonitrile mixtures, self-association of *n*-butanol through hydrogen bonding is remarkably promoted by the mixing with acetonitrile. With decreasing the acetonitrile contents, however, *n*-butanol self-associated clusters disintegrate completely. The interaction among *n*-butanol molecules changes from hydrogen bonding to dispersive, depending on the mixing ratio. When phenol is added as a solute to these binary mixtures, the solvation of phenol is found to be controlled by the solvent molecular clustering.

Introduction

When a substance is dissolved in a mixture of two or more solvents, the composition of its solvation shell may differ from that of the bulk solution. In this case the solute is said to be preferentially solvated by one solvent component.[1]

Preferential solvation phenomena depend not only on the physicochemical properties of solutes and solvents, but possibly also on the microheterogeneity in the solvent mixture itself: more specifically, solute species can favorably interact with self-associated components[2] or *clusters*. The extent of clustering is expected to depend on a variety of interactions balancing each other and resulting in different macroscopic behaviors.

On the basis of a mass spectrometric analysis[3,4] of such clusters, and consistently with NMR studies,[1] phenol in acetonitrile−water mixtures was reported to be preferentially solvated by acetonitrile molecules while the interaction of phenol with water only occurred at water mole fractions higher than 0.8. The effect of the acetonitrile−water mixing ratio on the formation of phenol hydrate clusters was found to be the same as that on the rate constant of hydrolysis of *tert*-butyl chloride in acetonitrile−water mixtures. This indicates that the interaction of weakly polar, hydrophobic substrates with water in acetonitrile−water mixtures is not only controlled by the solute−solvent interactions, but also by microheterogeneity of these mixtures.

The present study is aimed at determining whether solvation in binary mixtures of organic solvents is also influenced by the microheterogenity of the binary mixed solvents. In the course of this study we have examined the solvation of phenol (PhOH) in methanol−acetonitrile (MeOH−MeCN) and *n*-butanol−acetonitrile (BuOH−MeCN) mixtures at various molar ratios through a mass spectrometric analysis of clusters generated via fragmentation of liquid droplets. It will be shown that these two systems exhibit a markedly different behavior, which can be interpreted by taking into account the difference in the clustering structures of alcohols, in turn depending on their alkyl chain length and their mixing ratios.

Experimental Section

The molecular clusters, generated through fragmentation of liquid droplets via vacuum adiabatic expansion, were analyzed by a specially designed mass spectrometer (Figure 1). The principle of this method has been reported previously[4] and will be briefly recalled here. The sample solution is injected into a four-stage differentially pumped vacuum system (flow rate = 0.12 mL/min) through a nozzle whose temperature can be adjusted to within ±0.1 °C. The choice of the injection nozzle temperature (T_n) is crucial: in fact, the efficiency of formation of liquid droplets is smaller at lower temperatures since the liquid droplets beam is generated by a bubble jet system that performs best at appropriate temperatures only. In our samples, we found that signal detection is poor when T_n < 80 °C. On the other hand, if the temperature is too high (T_n > 130 °C), molecular clusters tend to fall away because of their excessive internal energy, thus mostly leading to detection of the parent species. Here we used a temperature range (100−110 °C) where spectral lines are little affected by the temperature changes. This temperature range depends on the flow rate and the physicochemical properties of the examined solution. Moreover, it is worth pointing out that the temperature of liquid droplets

* To whom correspondence should be addressed. E-mail: alessandro.bagno@unipd.it, akihiro-wakisaka@aist.go.jp.
[†] University of Padova.
[‡] Institute of Membrane Technology-CNR.

10.1021/jp037433j CCC: $27.50
Published on Web 02/18/2004

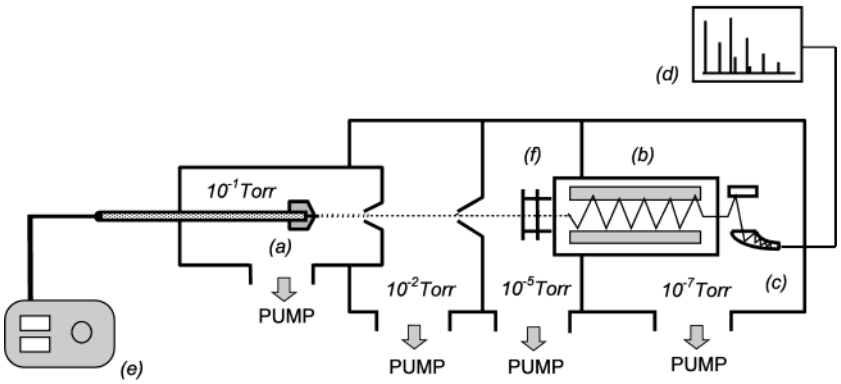

Figure 1. Sketch of the instrumentation for mass spectrometric analysis of clusters: (a) heater, (b) quadrupole filter, (c) amplifier, (d) oscilloscope, (e) HPLC pump, and (f) EI ionization.

undergoing adiabatic expansion is much lower than the nozzle temperature, with an estimated difference of 70−90 °C.[5]

Liquid droplets are formed in the first chamber at a pressure of 0.2 Torr and expanded to be fragmented into clusters in the second (1.0×10^{-2} Torr) and/or third chamber (1.0×10^{-5} Torr). The resulting clusters are ionized by electron impact (30 eV) in the third chamber and analyzed by a quadrupole mass spectrometer (Extrel C50-4000) in the fourth chamber (1.0×10^{-7} Torr). In this process, while the weakly interacting molecules leave the droplets, the more strongly interacting ones do not, and they appear as molecular clusters in the final mass spectrum. The composition of emerging clusters is then easily determined through a software-assisted mass analysis.

Binary mixtures at different mole fractions were prepared by weight and the concentration of PhOH was kept constant at 0.1 M for each sample.

Ab initio calculations were carried out with the Gaussian 98 program.[6] The basis-set superposition error was corrected for by means of the counterpoise method.[7]

Results

1. Mass Spectrometry of Clusters. *1.1. Alcohol−Acetonitrile Binary Mixtures.* Here we compare the structure of molecular clusters between MeOH−MeCN and BuOH−MeCN mixtures by means of the above-mentioned mass spectrometric analysis. By this comparison, it will be demonstrated that the cluster structures in the binary mixtures are controlled by the different size of the alkyl groups in MeOH and BuOH. Moreover, the cluster structures in the binary mixtures are not linearly dependent on the mixing ratio.

1.1.a. MeOH−MeCN Mixtures. To see the dependence of the cluster structures of MeOH−MeCN mixtures on the mixing ratio, the mass spectrometric analyses were performed for MeOH concentrations of 1, 5, 10, and 50 vol %. Figure 2 shows the mass spectra of clusters observed for the binary mixtures with MeOH concentrations of 1, 10, and 50 vol %. At 1 vol % of MeOH, the observed clusters are mainly composed of MeCN molecules (Figure 2a). As will be discussed later, the $H^+(MeCN)_n$ ($n = 2, 3, 4, ...$) clusters are probably formed by dipole−dipole interaction.

Increasing the MeOH concentration, the dipole−dipole interaction among acetonitrile molecules is perturbed. At 10 vol % of MeOH (Figure 2b), $H^+(MeCN)_n$ clusters with $n \geq 3$ are hardly formed. Instead, methanol clusters, $H^+(MeOH)_m$ ($m = 2, 3, 4, 5$), are formed prominently. Mixed clusters, $H^+(MeOH)_m(MeCN)_n$, are also formed.

At 50 vol % of MeOH, the observed clusters are exclusively composed of MeOH molecules (Figure 2c). Interestingly, the observed distribution of $H^+(MeOH)_m$ clusters is very similar to the distribution of the same clusters found in pure MeOH.

1.1.b. BuOH−MeCN Mixtures. Mass spectrometric analyses of BuOH−MeCN mixtures were performed for BuOH concentrations of 1, 5, 40, and 70 vol %. Figure 3 shows the mass spectra observed for 1, 40, and 70 vol % of BuOH.

At 1 vol % of BuOH (Figure 3a), $H^+(MeCN)_n$ clusters and $H^+(BuOH)_m(MeCN)_n$ clusters are formed. Upon increasing the BuOH concentration to 40 vol %, MeCN clusters are disintegrated and the formation of BuOH self-association clusters, $H^+(BuOH)_m$, is promoted, as shown in Figure 3b. However, the promotion of the BuOH self-association is remarkably decreased with a further increase of the BuOH concentration, as observed for 70 vol % of BuOH (Figure 3c).

1.2. Alcohol−Acetonitrile Binary Mixtures with Dissolved Phenol. To investigate how the difference between MeOH−MeCN and BuOH−MeCN cluster structures affects the solvation, mass spectrometric analyses for the binary mixtures including 0.1 M phenol (PhOH) were carried out. The concentration of the alcohols was varied as follows: 0, 1, 5, 10, 30, 50, 100 vol % of MeOH; 0, 1, 2, 20, 40, 50, 70, 80, 100 vol % of BuOH.

1.2.a. PhOH in MeOH−MeCN Mixtures. To compare the cluster structures in MeOH−MeCN mixtures with and without PhOH, Figure 4 shows the mass spectra of the PhOH−MeOH−MeCN system observed at the same vol % of MeOH as in Figure 2. Focusing on the clusters composed of PhOH and solvent molecules, they are found to be strongly dependent on the MeOH−MeCN mixing ratio. Thus, in the 1 vol % of MeOH solution (Figure 4a), PhOH−MeCN clusters are observed prominently among the clusters composed of PhOH and solvent (MeOH or MeCN) molecules. With increasing the MeOH concentration to 10 vol % (Figure 4b), PhOH−MeOH clusters become prominent instead of PhOH−MeCN clusters. The same phenomenon is observed in the 50 vol % of MeOH solution (Figure 4c). This indicates that the PhOH−MeOH interaction is more favorable than the PhOH−MeCN interaction even at low MeOH concentrations. The observed MeOH concentration dependence of the PhOH−MeOH interaction is in good agreement with the MeOH cluster formation in the MeOH−MeCN binary mixtures, as observed in Figure 2. Therefore, the existing clusters in the mixed solvent control the solvation of PhOH.

1.2.b. PhOH in BuOH−MeCN Mixtures. The observed mass spectra for PhOH−BuOH−MeCN at BuOH concentrations of 1, 40, and 70 vol % are shown in Figure 5. In the 1 vol % of BuOH solution (Figure 5a), the PhOH−BuOH interaction is comparable to the PhOH−MeCN interaction even though the BuOH concentration is much lower than that of MeCN. In the

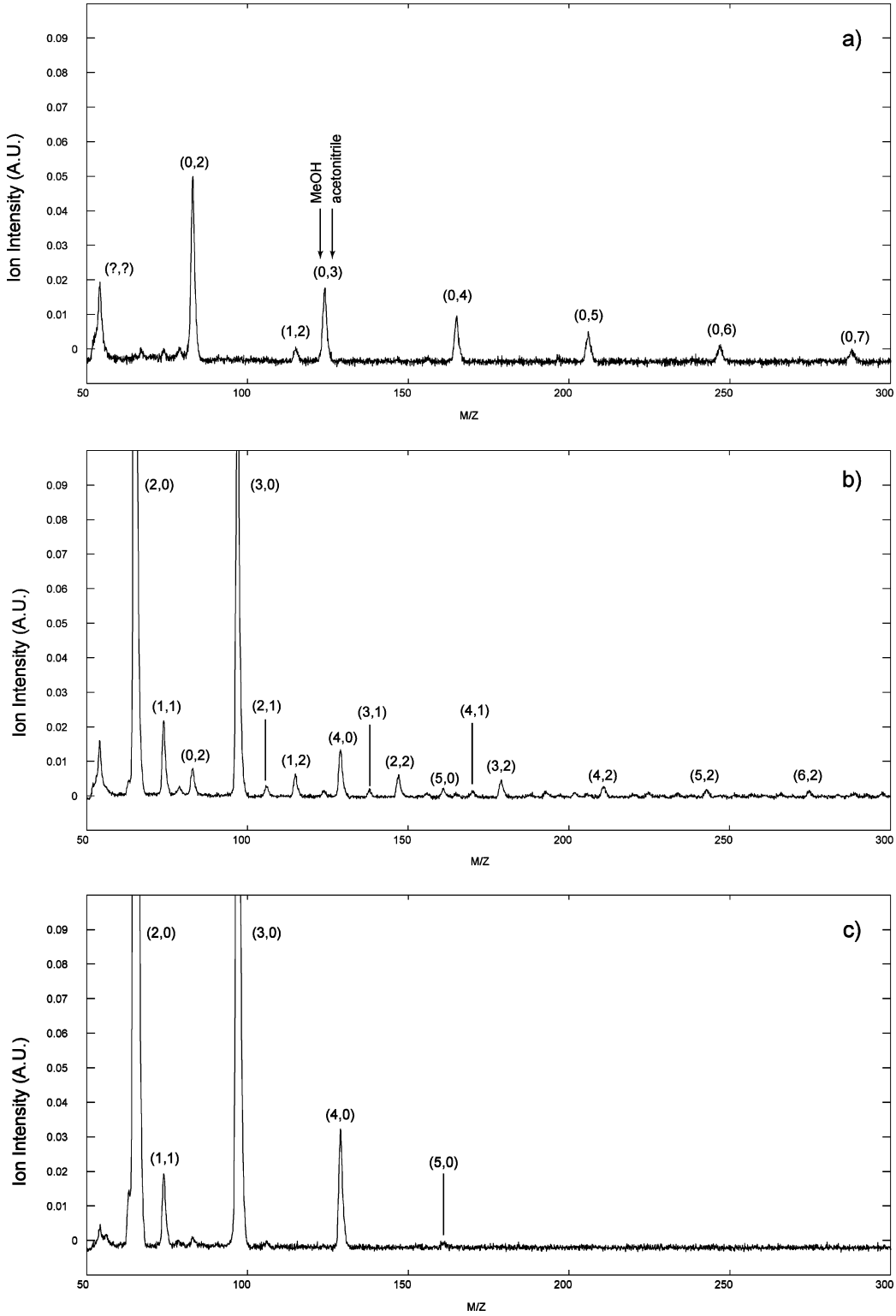

Figure 2. Mass spectra of the MeOH/MeCN system at various compositions: (a) 1 vol % of MeOH, (b) 10 vol % of MeOH, and (c) 50 vol % of MeOH. Each peak is superscripted by the number of molecules composing the cluster, as defined in panel a.

40 vol % of BuOH solution (Figure 5b), BuOH self-associated clusters, $H^+(BuOH)_m$, are predominantly observed, as in the same binary mixture without PhOH (Figure 3b). The solute PhOH in the 40 vol % of BuOH solution is mainly interacting with these $H^+(BuOH)_m$ clusters. In other words BuOH and PhOH molecules, which are separated from acetonitrile, form clusters favorably.

In the 70 vol % of BuOH solution (Figure 5c), however, PhOH−BuOH clusters disappear almost completely. This behavior is similar to that observed for BuOH−MeCN mixtures seen before, but strikingly at variance with that of MeOH−MeCN mixtures. The reasons for this will be discussed below.

2. Data Treatment and Processing. For all samples, data collection was carried out under identical conditions, as reported in the Experimental Section. A dedicated postprocessing was then employed on such data, to reveal the clustering properties of observed mixtures in a more compact form. Thus, the intensity ratios of the clusters composed of PhOH and alcohol

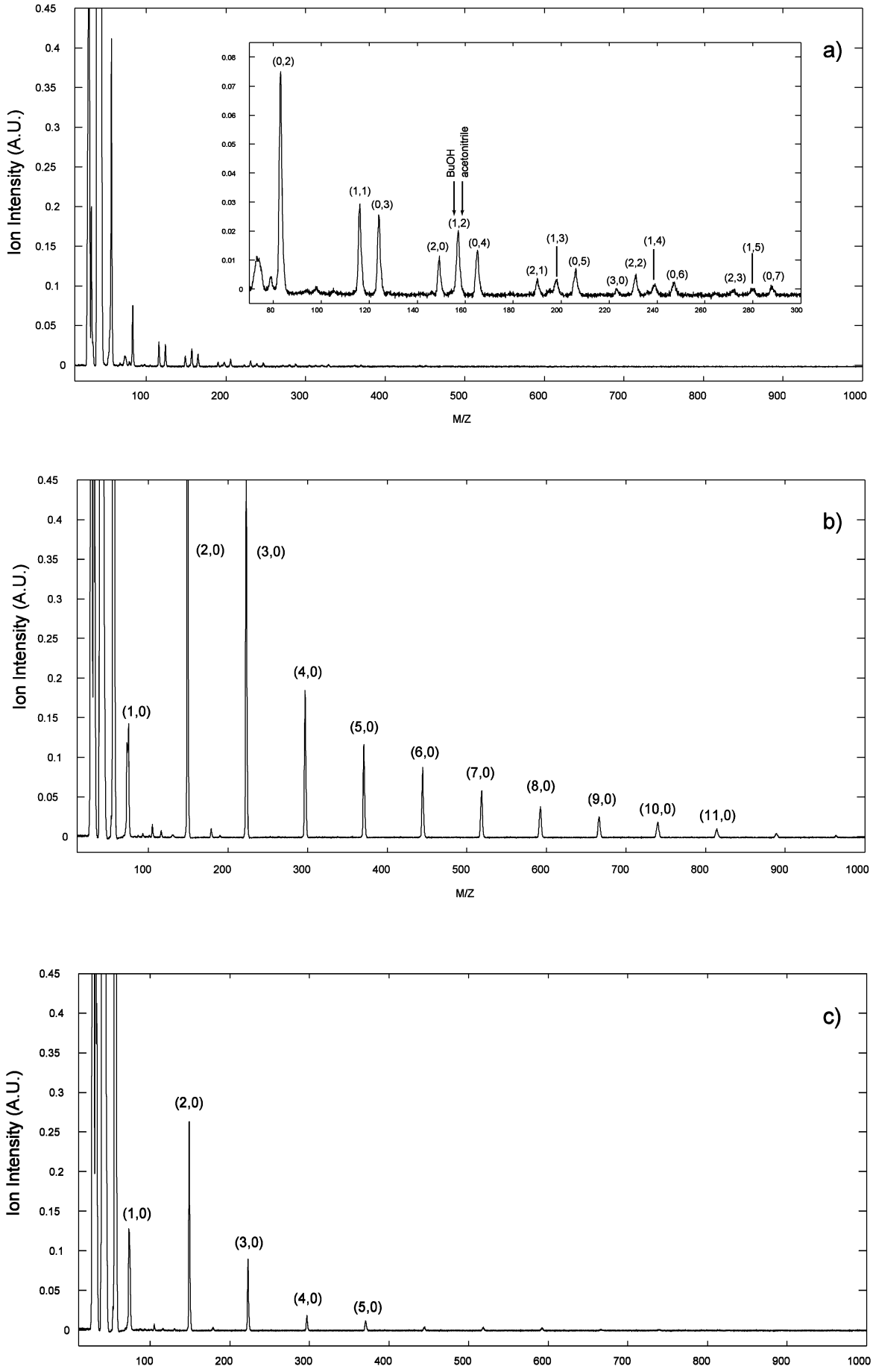

Figure 3. Mass spectra of the BuOH/MeCN system at various compositions: (a) 1 vol % of BuOH, (b) 40 vol % of BuOH, and (c) 70 vol % of BuOH. See caption to Figure 2.

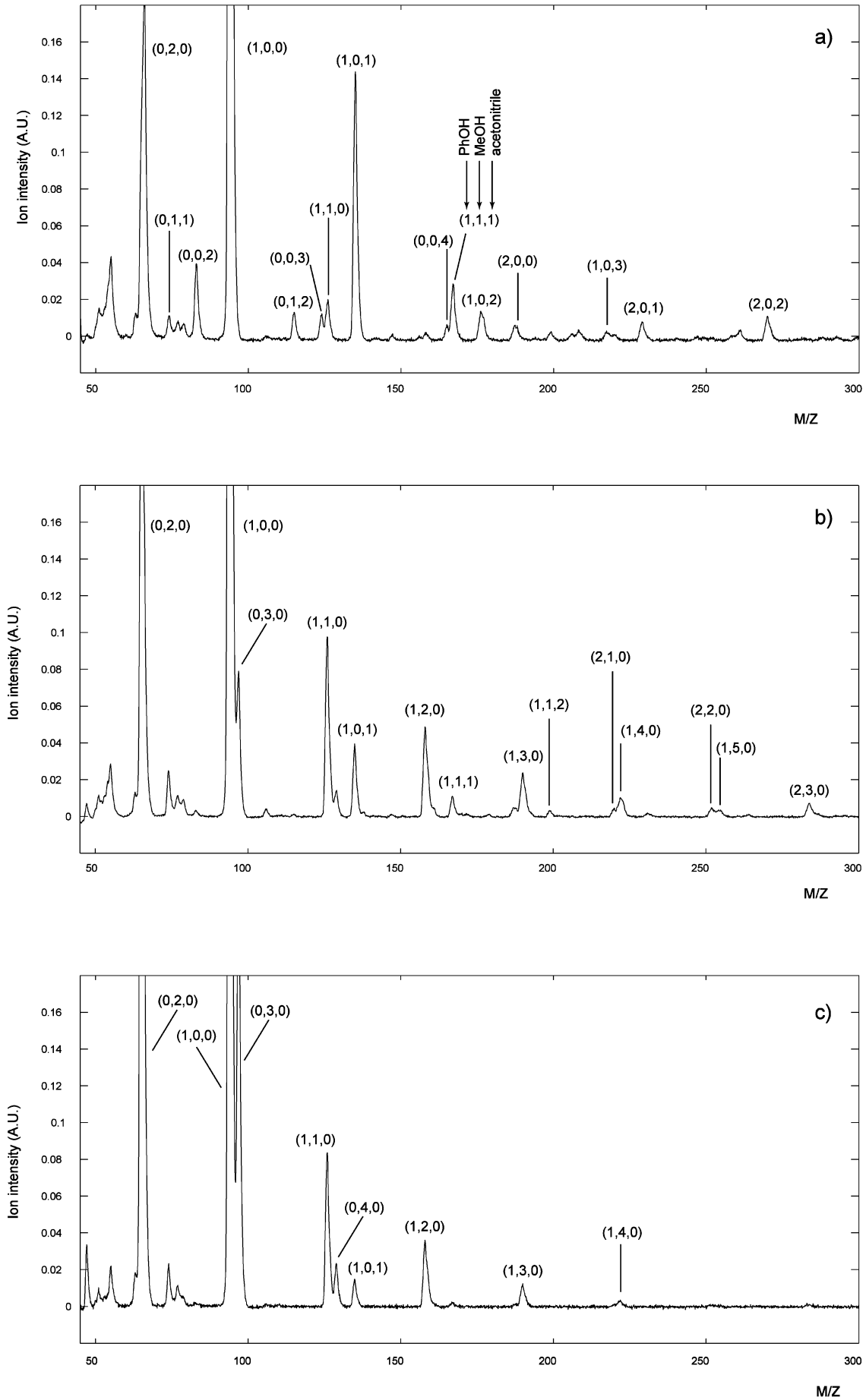

Figure 4. Mass spectra of the MeOH/MeCN system at various compositions, with dissolved PhOH (0.1 M): (a) 1 vol % of MeOH, (b) 10 vol % of MeOH, (c) 50 vol % of MeOH. See caption to Figure 2.

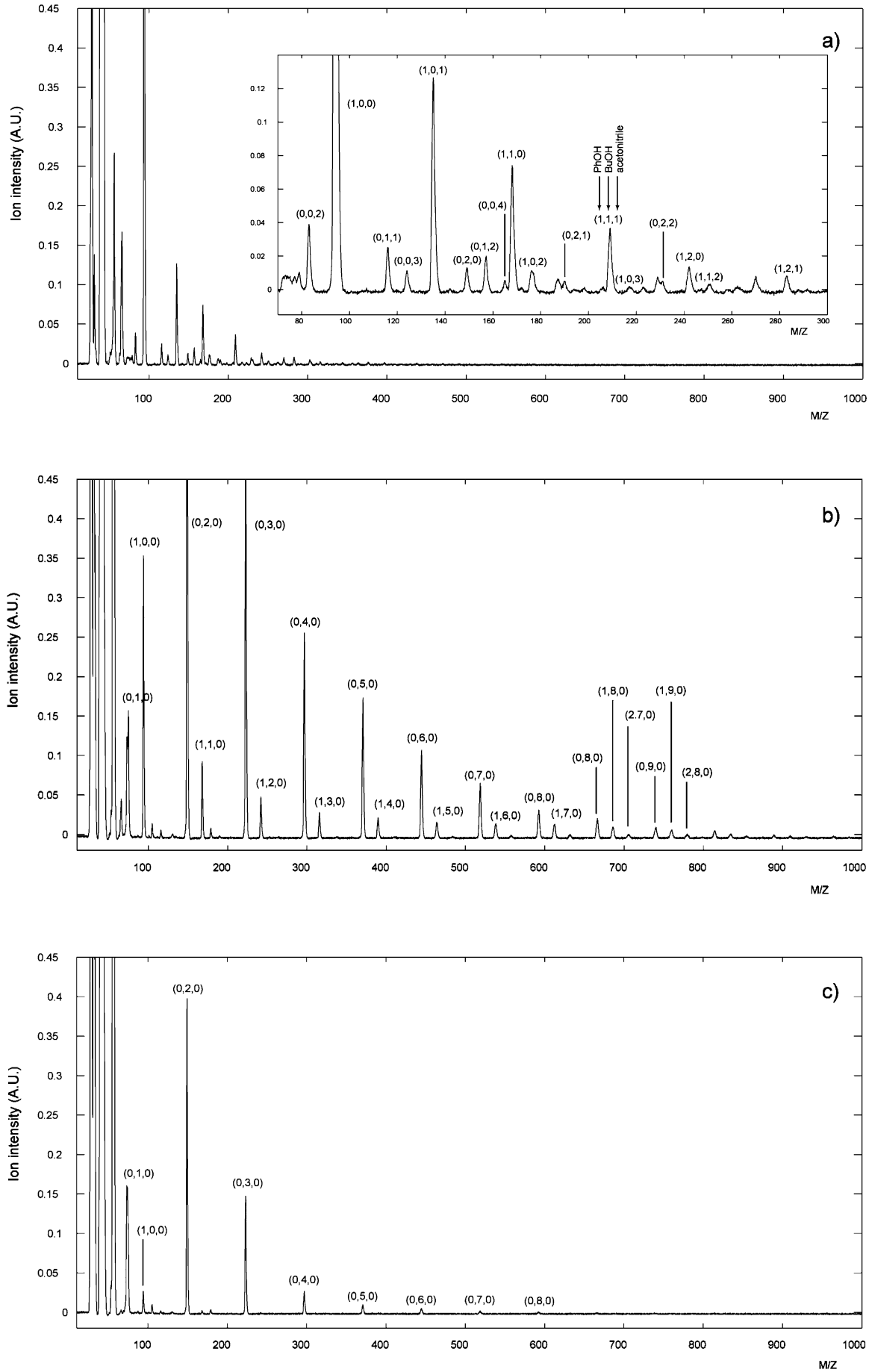

Figure 5. Mass spectra of the BuOH/MeCN system at various compositions, with dissolved PhOH (0.1 M): (a) 1 vol % of BuOH, (b) 40 vol % of BuOH, and (c) 70 vol % of BuOH. See caption to Figure 2.

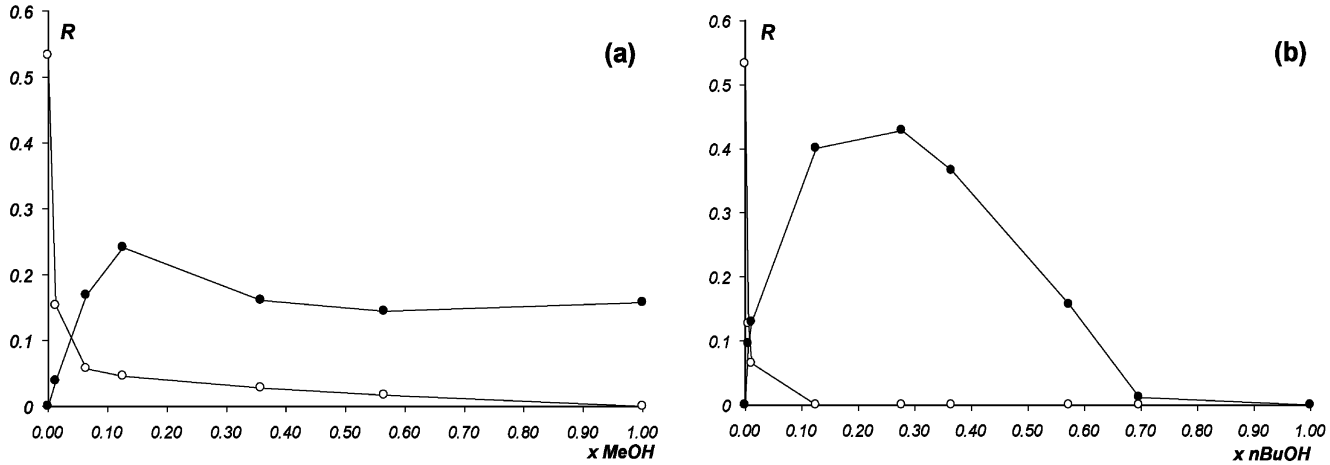

Figure 6. Plots of $R_{(PhOH)}$ as a function of alcohol mole fraction: (a) MeOH−MeCN and (b) BuOH−MeCN. Filled circles: $R(PhOH)_{ROH}$; open circles: $R(PhOH)_{MeCN}$. PhOH concentration is 0.1 M in each sample.

to all the clusters including PhOH, $R(PhOH)_{ROH}$, are calculated by eq 1 on the basis of the observed mass spectra. Similarly,

$$R(\mathrm{PhOH})_{\mathrm{ROH}} = \frac{\sum_m I_{\mathrm{PhOH(ROH)}_m}}{I_{(\mathrm{PhOH})} + \sum_m I_{\mathrm{PhOH(ROH)}_m} + \sum_n I_{\mathrm{PhOH(MeCN)}_n} + \sum_{m,n} I_{\mathrm{PhOH(ROH)}_m\mathrm{(MeCN)}_n}} \quad (1)$$

the intensity ratios of the clusters composed of PhOH and MeCN to all the clusters including PhOH, $R(PhOH)_{MeCN}$, are calculated by eq 2, where I_x represents the peak intensity of cluster x, and

$$R(\mathrm{PhOH})_{\mathrm{MeCN}} = \frac{\sum_n I_{\mathrm{PhOH(MeCN)}_n}}{I_{(\mathrm{PhOH})} + \sum_m I_{\mathrm{PhOH(ROH)}_m} + \sum_n I_{\mathrm{PhOH(MeCN)}_n} + \sum_{m,n} I_{\mathrm{PhOH(ROH)}_m\mathrm{(MeCN)}_n}} \quad (2)$$

ROH corresponds to MeOH or BuOH. The $R(PhOH)_{ROH}$ and $R(PhOH)_{MeCN}$ values are plotted against the alcohol mole fractions (x_{MeOH} and x_{BuOH}) in Figure 6.

An analogous function R_k' is introduced to account for generation of alcohol clusters larger than k units in binary mixtures *without* dissolved phenol:

$$R_k' = \frac{\sum_{n=k} I_{(\mathrm{ROH})_n}}{\sum_{n=2} I_{(\mathrm{ROH})_n}} \quad (3)$$

In summary, a plot of R (Figure 6a,b) or R_k' vs x_{ROH} gives the relative population of specific cluster families as a function of the composition of the mixture. As is apparent from the figures, the R function never reaches unit values: this is mainly due to the presence of strong parent phenol signals which contribute significant $I_{(PhOH)}$ values to eqs 1 and 2. These signals may be generated either by isolated phenol molecules or by cluster-desolvated phenol, as a consequence of the electron impact process.

In the MeOH−MeCN mixtures (Figure 6a), the $R(PhOH)_{MeCN}$ and $R(PhOH)_{MeOH}$ values rapidly decrease and increase, respectively, by increasing x_{MeOH} up to 0.1. In the region of $x_{MeOH} > 0.1$, $R(PhOH)_{MeOH}$ and $R(PhOH)_{MeCN}$ are almost constant with the increase of x_{MeOH}. This indicates that the microscopic environment around the PhOH molecule in the MeOH−MeCN mixture is sensitive to the MeOH−MeCN mixing ratio mostly when $0 < x_{MeOH} < 0.1$, and that PhOH is preferentially interacting with MeOH for $x_{MeOH} > 0.1$, where the PhOH−MeOH interaction looks similar to that in pure MeOH solvent.

In the BuOH−MeCN mixtures (Figure 6b), $R(PhOH)_{MeCN}$ and $R(PhOH)_{BuOH}$ values rapidly decrease and increase, respectively, with increase of x_{BuOH} up to 0.1, similar to the MeOH−MeCN system. However, the $R(PhOH)_{BuOH}$ values show a maximum around $x_{BuOH} = 0.2-0.3$ and drop with further increasing x_{BuOH}. This suggests some kind of reorganization of BuOH molecules in the solution.

3. Energetics of Dispersive and Dipole−Dipole Interactions Based on ab Initio Calculations. The energetics of dispersive interactions among alkyl chains of the alcohols has been investigated by means of ab initio calculations on MeOH and BuOH dimers. To exclude hydrogen-bonding contributions to the potential energy surface, the dimers were deliberately arranged in a head-to-tail configuration. As a consequence, the potential energy wells presented below do not refer to absolute energetic minima, which would be otherwise reached in intermolecular arrangements appropriate also for the formation of hydrogen bonds. Rather, these potential energy plots should be taken as an estimate of the energetics of the other, weaker interactions occurring in these systems. The dipole−dipole interaction in a MeCN dimer was also investigated, with the two molecules arranged in a geometry taken from ref 8.

After optimization of the monomer geometries at the B3LYP/6-31G(d,p) level, calculations have been carried out at the MP2/cc-pVTZ level of theory and corrected for the basis-set superposition error. The resulting potential energy as a function of the intermolecular distance R (as defined in Figure 7) is shown in Figure 8.

Discussion

We will first survey the intermolecular interactions available to the studied systems, i.e., dipole−dipole (DD), hydrogen-bonding (HB), and dispersive interactions. To this purpose, some relevant physical properties, which are useful to estimate the magnitude of the aforementioned interactions, are collected in Table 1. In particular, the parameters α_2^H and β_2^H refer to HB acidity and basicity, while the dipole moment μ and the polarizability α are related to DD and dispersive interactions, respectively. From Table 1 it is apparent that (a) all alcohols are medium to strong HB donors and acceptors; (b) the dipole

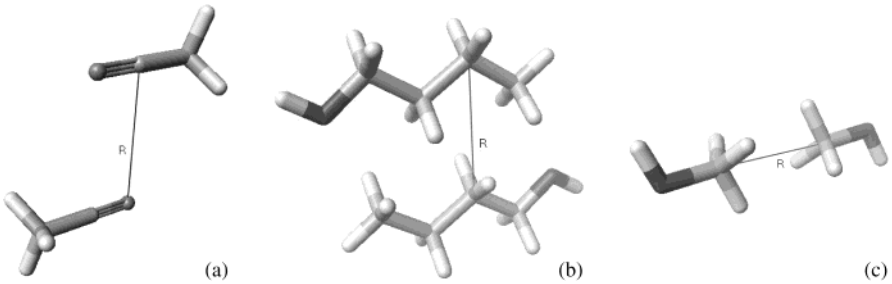

Figure 7. Geometry of the dimers investigated by ab initio calculations: (a) acetonitrile; (b) butanol; and (c) methanol. The distance *R* is measured as indicated.

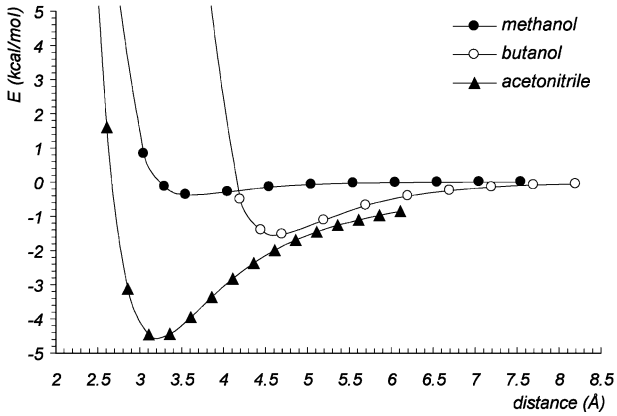

Figure 8. Potential energy (kcal/mol) as a function of *R* (Å; see Figure 7) for MeOH, BuOH, and MeCN dimers.

TABLE 1: Physical Properties Implicated in Intermolecular Interactions of the Studied Molecules

species	α_2^H [a]	β_2^H [a]	μ (D)[b]	α (10^{-24} cm^3)[b]
phenol	0.6	0.3	1.22	11.1
methanol	0.43	0.47	1.70	3.3
n-butanol	0.37	0.48	1.66	8.9
acetonitrile	0.07	0.32	3.92	4.5

[a] Hydrogen-bonding acidity (α_2^H) and basicity (β_2^H); definitions and data from ref 9. [b] Data from ref 10.

moment of acetonitrile is much larger than that of all other molecules; and (c) the polarizabilities decrease in the order phenol > butanol > acetonitrile > methanol, as expected on the basis of their molecular weights and implying that the magnitude of dispersive interactions will increase correspondingly. These data indicate acetonitrile and butanol as the strongest solvent partners involved in DD and dispersive interactions, respectively.

1. Dipole−Dipole Interactions. As was previously noted, a monotonic decrease upon increasing x_{ROH} is observed in the population of PhOH−MeCN clusters for both examined systems. This behavior may be accounted for by postulating that the interactions responsible for the formation of acetonitrile clusters are the same all through the explored concentration range. The nature of such interactions is suggested by results from X-ray diffraction and IR data in liquid acetonitrile,[8] which have been interpreted on the basis of acetonitrile domains (clusters) which maximize their DD stabilization energy through a zigzag arrangement. When such an arrangement is considered for the acetonitrile dimer, our ab initio calculations show a maximum stabilization energy of ca. 4.8 kcal/mol. On the other hand, the dipole moment of the alcohols is much smaller, so that DD stabilization is expected to be less important than hydrogen bonding. It should be emphasized that the seemingly larger stabilization of the MeCN dimer compared to that of the alcohols is only due to the neglect of HB between alcohol molecules, which is much stronger (see below).

2. Hydrogen-Bonding Interactions. In both mixed media, the amount of detected PhOH−ROH clusters (R = Me or Bu) is, on average, larger than that of the corresponding PhOH−MeCN clusters: this behavior is attributed to an efficient hydrogen bonding occurring between such molecules. Hydrogen bonding is presumably the strongest available interaction, but it can only take place when two molecules both possess suitable donor−acceptor capabilities and approach each other in specific orientations. The tendency toward an HB dimerization can be quantitatively expressed by means of empirical scales, such as those developed by Abraham[9] in terms of two parameters (α_2^H and β_2^H) describing respectively the HB acidity and HB basicity of a given species (Table 1). These parameters can be employed to estimate the equilibrium constants for HB dimerization of specific donor−acceptor pairs in an inert solvent (eq 4):

$$A{-}H + B \overset{K}{\rightleftharpoons} A{-}H\cdots B$$

$$\log K = 7.354\alpha_2^H(A)\beta_2^H(B) - 1.094 \qquad (4)$$

The resulting equilibrium constants clearly show that log *K* values for PhOH−BuOH (1.02) and PhOH−MeOH (0.98) are larger than that for PhOH−MeCN (0.32). Thus, PhOH forms hydrogen bonds with alcohol molecules more favorably than with acetonitrile. However, although the log *K* values for PhOH−BuOH and PhOH−MeOH are very similar, the dependence of the PhOH−alcohol clustering on the alcohol−acetonitrile mixing ratio is clearly different in MeOH−MeCN and in BuOH−MeCN, as shown in Figure 6. This suggests that the overall PhOH−alcohol interaction depends not only on the HB strength, but also on the molecular clustering, which is controlled by the alcohol−acetonitrile mixing ratio. Equation 4 also allows similar values to be estimated for the HB of PhOH (donor) with BuOH and MeOH (acceptors), implying that PhOH can serve as a "neutral" probe to investigate the clustering properties of our alcohol/acetonitrile mixtures.

Finally, we note that the HB between two MeCN molecules is not favorable (log $K = -0.93$), thus validating the previous assumption that DD is the most important interaction for MeCN association.

3. Dispersive Interactions. Unlike DD and HB, dispersive interactions are effective also in nonspecific intermolecular arrangements, as long as the polarizabilities are sufficiently large. To get at least a semiquantitative estimate, dispersive interactions between alcohol molecules have been obtained by ab initio calculations (Figure 8). These reveal an appreciable stabilization energy (up to 1.5 kcal/mol) for the BuOH dimer, mainly attributable to dispersion forces between alkyl chains. By comparison, two MeOH molecules gain a much smaller stabilization (ca. 0.3 kcal/mol) from purely dispersive interactions and therefore are more likely to interact via hydrogen bonding, whose energy reaches 7.6 kcal/mol in the dimer

species.[11] In fact, the liquid structure of pure MeOH is often described in terms of competition between close-packing of methyl groups and hydrogen bonding of hydroxyl groups:[12] rings and branched rings held together by $[\cdots O-H\cdots O-H]_n$ frames are the most common clustered structures found not only in pure liquid MeOH, but in MeOH−water mixtures as well.[13] In our binary mixtures MeCN is likely to terminate methanol OH chains, thus decreasing the size of MeOH homoclusters. Yet, the evidence of MeOH clusters throughout the observed mass spectra suggests that HB is still the most efficient mechanism of cluster formation, at least from an energetic point of view.

4. Clustering Depending on the Alcohol−Acetonitrile Mixing Ratio. As for the MeOH−MeCN binary mixtures, MeOH molecules form $H^+(MeOH)_m$ clusters through hydrogen-bonding interaction. Therefore, such clusters survive after the adiabatic expansion in the vacuum chambers of the mass spectrometer. As Figure 2 shows, the $H^+(MeOH)_m$ clusters become prominent at MeOH concentrations >10 vol % instead of the acetonitrile dipole−dipole interacting clusters. Interestingly, the mass distribution of the MeOH clusters observed at the MeOH concentrations >10 vol % is similar to that observed in pure MeOH. The self-association of MeOH is hardly promoted by the mixing with MeCN in these mixing ratios. In other words, cluster formation takes place by the same hydrogen-bonding mechanism throughout the observed concentration range and the relatively strong MeOH−MeOH interaction in the binary mixture is not influenced by the presence of acetonitrile. On the other hand, the clustering of MeCN is drastically depressed by mixing with methanol.

In the case of BuOH−MeCN mixtures, the main difference from MeOH−MeCN mixtures lies in the sharp drop in the population of BuOH self-association clusters at $x_{BuOH} > 0.2$. Furthermore, as shown in Figure 3, self-association of BuOH is remarkably promoted by the mixing with MeCN. This effect of MeCN on the self-association of BuOH is maximum when x_{BuOH} is ca. 0.2. With increasing the BuOH contents in the mixture, the formation of the BuOH self-associated clusters is drastically decreased. At higher BuOH contents, weaker dispersive interaction among the alkyl chain will take over, implying a major rearrangement in the cluster structure. As for the reason such rearrangement takes place depending on the BuOH−MeCN mixing ratio, we propose the following rationale.

The HB between BuOH and MeCN is not very strong ($\log K = -0.22$), which presumably makes the dispersive interaction an important competing factor. However, there is a large size mismatch between BuOH and MeCN, which renders this heteroassociation also relatively inefficient, and in turn favors the formation of self-associated BuOH clusters rather than mutual solvation. At low BuOH concentrations, these clusters are mainly stabilized by hydrogen-bonded networks. At higher BuOH concentrations, where BuOH clusters are likely to be surrounded by other BuOH molecules, it becomes less and less feasible to arrange several BuOH molecules to form an extended hydrogen-bonded network. It is interesting that the formation of large hydrogen-bonded clusters is possible in a limited range of BuOH concentrations: this may represent a microscopic phase separation within this region.

Mandal et al.[14] showed that, in the case of pure methanol, the enthalpy of activation ΔH_e for low-frequency dielectric relaxation is of the magnitude needed to break 1 mol of hydrogen bonds, owing to the absence of interlocking chains. Upon going from methanol to butanol, ΔH_e doubles and this behavior cannot be explained by strengthening of intermolecular HB upon increasing the chain length (in fact, IR measurements suggest no change in strength). The authors claim that the progressive increase of ΔH_e with increasing chain length is rather to be sought in the chain itself and, more precisely, in the dispersive interactions of one chain with another, hence in line with the above discussion.

In consideration with the molecular clustering in the binary mixtures MeOH−MeCN and BuOH−MeCN, the PhOH−alcohol hydrogen-bonding interaction in these binary mixtures is found to be controlled by the clustering structures of the binary mixtures.

Machado and co-workers have recently investigated the preferential solvation of pyrene in alcohol/acetonitrile mixtures.[15] It has been found that this nonpolar, strongly hydrophobic solute exhibits an increasing preference for longer -chain alcohols (i.e., methanol < ethanol < propanol < butanol). This result agrees with our hypothesis: in BuOH−MeCN mixtures, pyrene is drawn from acetonitrile to a more hydrophobic environment provided by the butanol self-associated clusters.

Conclusions

On the basis of a mass spectrometric analysis for MeOH−MeCN and BuOH−MeCN mixtures including PhOH as a solute, we conclude that PhOH favorably interacts with self-associated alcohol molecules in the mixtures. In BuOH−MeCN mixtures, the microscopic structures are reorganized from hydrogen-bonded structures to flexible structures interacting through dispersion forces upon varying the mixing ratio. On the other hand, in the MeOH−MeCN mixtures, methanol clusters always form through hydrogen bonding. The clustering in the binary mixed solvent sensitively influences the solvation of PhOH.

Acknowledgment. Financial support from AIST, Tsukuba to F.R. is gratefully acknowledged.

References and Notes

(1) (a) Bagno, A.; Scorrano, G.; Stiz, S. *J. Am. Chem. Soc.* **1997**, *119*, 2299. (b) Bagno, A.; Campulla, M.; Pirana, M. *Chem. Eur. J.* **1999**, *5*, 1291.

(2) Shin, D. N.; Wijnen, J. W.; Engberts, J. B. F. N.; Wakisaka, A. *J. Phys Chem. B* **2001**, *105*, 6759.

(3) Wakisaka, A.; Shimiza, Y.; Nishi, N.; Tokumaru, K.; Sakuragi, S. *J. Chem. Soc., Faraday Trans.* **1992**, *88*, 1129.

(4) Wakisaka, A.; Takahashi, S.; Nishi, N. *J. Chem. Soc., Faraday Trans.* **1995**, *91*, 4063.

(5) Nishi, N.; Yamamoto, K. *J. Am. Chem. Soc.* **1987**, *109*, 7353.

(6) Frisch, M. J.; Trucks, G. W.; Schlegel, H. B.; Scuseria, G. E.; Robb, M. A.; Cheeseman, J. R.; Zakrzewski, V. G.; Montgomery, J. A., Jr.; Stratmann, R. E.; Burant, J. C.; Dapprich, S.; Millam, J. M.; Daniels, A. D.; Kudin, K. N.; Strain, M. C.; Farkas, O.; Tomasi, J.; Barone, V.; Cossi, M.; Cammi, R.; Mennucci, B.; Pomelli, C.; Adamo, C.; Clifford, S.; Ochterski, J.; Petersson, G. A.; Ayala, P. Y.; Cui, Q.; Morokuma, K.; Malick, D. K.; Rabuck, A. D.; Raghavachari, K.; Foresman, J. B.; Cioslowski, J.; Ortiz, J. V.; Stefanov, B. B.; Liu, G.; Liashenko, A.; Piskorz, P.; Komaromi, I.; Gomperts, R.; Martin, R. L.; Fox, D. J.; Keith, T.; Al-Laham, M. A.; Peng, C. Y.; Nanayakkara, A.; Gonzalez, C.; Challacombe, M.; Gill, P. M. W.; Johnson, B.; Chen, W.; Wong, M. W.; Andres, J. L.; Gonzalez, C.; Head-Gordon, M.; Replogle, E. S.; Pople, J. A. *Gaussian 98*, revision A.11; Gaussian, Inc.: Pittsburgh, PA, 1998.

(7) Boys, S. F.; Bernardi, F. *Mol. Phys.* **1970**, *19*, 553.

(8) Takamaku, T.; Tabata, M.; Yamaguchi, T.; Nishimoto, J. *J. Phys. Chem. B* **1998**, *102*, 8880.

(9) Abraham, M. H. *Chem. Soc. Rev.* **1993**, 73.

(10) *CRC Handbook of Chemistry and Physics*; Lide, D. R., Ed.; CRC Press: Boca Raton, FL, 1997.

(11) Hibbert, F.; Emsley, J. *Adv. Phys. Org. Chem.* **1990**, *26*, 256.

(12) El-Shall, M. S.; Wright, D.; Ibrahim, Y.; Mahmoud, H. *J. Phys. Chem. A* **2003**, *107*, 5933.

(13) Guo, J.-H.; Luo, Y.; Augustsson, A.; Kashtanov, S.; Rubensson, J.-E.; Shuh, D. K.; Ågren, H.; Nordgren, J. *Phys. Rev. Lett.* **2003**, *91* (15), 157401.

(14) Mandal, H.; Frood, D. G.; Saleh, M. A.; Morgan, B. K.; Walker, S. *Chem. Phys.* **1989**, *134*, 441.

(15) Silva, M. A. R.; da Silva, D. C.; Machado, V. G.; Longhinotti, E.; Frescura, V. L. A. *J. Phys. Chem. A* **2002**, *106*, 8820.